Renal intercalated cells are rather energized by a proton than a sodium pump

Régine Chambrey[a,1,2], Ingo Kurth[b,1], Janos Peti-Peterdi[c], Pascal Houillier[d,e], Jeffrey M. Purkerson[f], Françoise Leviel[d,e], Moritz Hentschke[g], Anselm A. Zdebik[h], George J. Schwartz[f], Christian A. Hübner[b,3], and Dominique Eladari[a,d,2,3]

[a]Institut National de la Santé et de la Recherche Médicale, Unité Mixte de Recherche de Santé 872, Centre de Recherche Paris Centre de Recherche des Cordeliers, Faculté de Médecine Paris Descartes, Sorbonne Paris Cité, F-75006 Paris, France; [b]Jena University Hospital, Institute of Human Genetics, D-07743 Jena, Germany; [c]Departments of Physiology and Biophysics, and Medicine, Zilkha Neurogenetic Institute, University of Southern California, Los Angeles, CA 90033; [d]Département de Physiologie, Assistance Publique–Hôpitaux de Paris, Hôpital Européen Georges Pompidou, F-75015 Paris, France; [e]Centre de Recherche des Cordeliers, Institut National de la Santé et de la Recherche Médicale Unité 872, Faculté de Médecine Paris Descartes, Sorbonne Paris Cité, F-75006 Paris, France; [f]Division of Pediatric Nephrology, University of Rochester, Rochester, NY 14642; [g]University Medical Center Hamburg-Eppendorf, Institute of Medical Microbiology, Virology and Hygiene, 20246 Hamburg, Germany; and [h]Departments of Neuroscience, Physiology and Pharmacology and Medicine, University College London, London NW3 2PF, UK

Edited* by Gerhard Giebisch, Yale University School of Medicine, New Haven, CT, and approved March 21, 2013 (received for review December 19, 2012)

The Na^+ concentration of the intracellular milieu is very low compared with the extracellular medium. Transport of Na^+ along this gradient is used to fuel secondary transport of many solutes, and thus plays a major role for most cell functions including the control of cell volume and resting membrane potential. Because of a continuous leak, Na^+ has to be permanently removed from the intracellular milieu, a process that is thought to be exclusively mediated by the Na^+/K^+-ATPase in animal cells. Here, we show that intercalated cells of the mouse kidney are an exception to this general rule. By an approach combining two-photon imaging of isolated renal tubules, physiological studies, and genetically engineered animals, we demonstrate that inhibition of the H^+ vacuolar-type ATPase (V-ATPase) caused drastic cell swelling and depolarization, and also inhibited the NaCl absorption pathway that we recently discovered in intercalated cells. In contrast, pharmacological blockade of the Na^+/K^+-ATPase had no effects. Basolateral NaCl exit from β-intercalated cells was independent of the Na^+/K^+-ATPase but critically relied on the presence of the basolateral ion transporter anion exchanger 4. We conclude that not all animal cells critically rely on the sodium pump as the unique bioenergizer, but can be replaced by the H^+ V-ATPase in renal intercalated cells. This concept is likely to apply to other animal cell types characterized by plasma membrane expression of the H^+ V-ATPase.

proton pump | plasma membrane | ion transporter

The ionic composition of the intracellular milieu is kept different from the surrounding medium at a large cost of metabolic energy. Ion transport contributes as much as 25–45% of total cellular oxygen consumption and heat production. Indeed, the maintenance of the steady-state ionic composition expends such a large fraction of cellular metabolism that the concept of ion transport as a "pacemaker of cellular metabolism" was developed (1–3). The explanation is a continuous leak of sodium ions into the cytoplasm, which leads to incessant transport, and hence, ATP hydrolysis by the ion motive ATPases.

In animal cells the Na^+/K^+ P-type ATPase (P-ATPase) is thought to generate the sodium gradient that energizes the transport of a variety of solutes including sugars, amino acids, and other metabolites needed for absorption and excretion of nutrients and waste products (4). Intercalated cells (ICs), a cell type that is widely distributed in all vertebrate phyla and has a variety of names, chloride cells, mitochondria-rich cells, or ICs (5), may be an exception to this general rule. These cells are specialized for proton transport, and we show here that they do not contain any detectable Na^+/K^+ P-ATPase activity but transport protons to couple metabolism and ion transport. Furthermore, some of these cells are capable of NaCl absorption (6), but here the transported moieties are also coupled to proton transport.

The proton pump expressed by these cells, the H^+ vacuolar-type ATPase (V-ATPase), is related to the F_0F_1 ATP-synthase of mitochondria (7, 8). In cells like, for example, epididymal narrow and clear cells, osteoclasts, cells of the endolymphatic epithelium in the inner ear, and renal ICs, the H^+ V-ATPase mediates active acidification of the extracellular medium. In mammalian kidney, the H^+ V-ATPase is also required for chloride absorption via ICs (9, 10). In addition, in some species like freshwater fishes or batrachians, the H^+ V-ATPase has been proposed to drive Na^+ uptake (11, 12). Nevertheless, in all these cells the role of the Na^+/K^+ P-ATPase has never been questioned because the Na^+ pump is thought to be indispensable for sodium extrusion out of the cell, and hence, for proper regulation of cell volume or membrane voltage.

Here, we show that the H^+ V-ATPase controls the steady-state cell volume and membrane potential difference in mouse renal ICs as well as the transepithelial sodium and chloride transport through these cells, functions that previously have been ascribed to be part of the cardinal repertoire of cells containing the Na^+/K^+ P-ATPase.

Results

H^+ V-ATPase Controls Steady-State Cell Volume and Resting Membrane Potential of Renal β-ICs. The ICs of the kidney are located in a distal segment, the collecting duct, which also contains principal cells (13). ICs are specialized for H^+ and HCO_3^- transport. They are enriched with mitochondria and have a high cytoplasmic content of carbonic anhydrase II (14). Two functionally distinct subtypes of ICs have been identified in the cortical collecting duct (CCD): the β-ICs secrete HCO_3^-, whereas the α-ICs secrete H^+. An apical Cl^-/HCO_3^- exchanger and a basolateral H^+ V-ATPase mediate secretion of base by the β-ICs, whereas α-ICs secrete acid by an apical H^+ V-ATPase and a basolateral Cl^-/HCO_3^- exchanger. In both cell types, it is the same H^+ V-ATPase that is located either in the apical membrane of the α-ICs or in the basolateral membrane of the β-ICs (15). However, there is now general agreement that the apical

Author contributions: R.C., I.K., G.J.S., C.A.H., and D.E. designed research; R.C., I.K., J.P.-P., P.H., J.M.P., F.L., M.H., A.A.Z., and G.J.S. performed research; R.C., I.K., J.P.-P., P.H., J.M.P., F.L., M.H., A.A.Z., G.J.S., C.A.H., and D.E. analyzed data; and R.C., I.K., C.A.H., and D.E. wrote the paper.

The authors declare no conflict of interest.

*This Direct Submission article had a prearranged editor.

[1]R.C. and I.K. contributed equally to this work.

[2]Previous address: Institut National de la Recherche et de la Santé, Unité Mixte de Recherche 970 (Equipe 3), Paris Cardiovascular Research Center, F-75015 Paris, France.

[3]To whom correspondence may be addressed. E-mail: dominique.eladari@inserm.fr or christian.huebner@mti.uni-jena.de.

This article contains supporting information online at www.pnas.org/lookup/suppl/doi:10.1073/pnas.1221496110/-/DCSupplemental.

Cl^-/HCO_3^- exchanger of the β-IC is pendrin (16), whereas the basolateral exchanger of the α-ICs is a variant of the red cell anion exchanger 1 (Ae1) (17).

All living cells contain impermeable anionic colloids, which are mostly made up of proteins and organic phosphates. As a result of this, there is a high concentration of nondiffusible anions across the cell membrane, thus generating significant osmotic force between extracellular and intracellular compartments, also known as the Donnan effect. In typical animal cells, the Na^+/K^+ P-ATPase creates steep gradients for Na^+ and K^+ across the plasma membrane. Because the plasma membrane has a higher permeability for K^+ over Na^+ and anions, an outwardly directed K^+ leak creates an inside-negative membrane potential. In cells that use a proton pump as bioenergizer, like plant and fungi cells, active expulsion of protons by the pump directly generate an inside-negative membrane potential. In both cases, the inside-negative membrane potential is critical to maintain steady-state cell volume because it drives a steady flow of inorganic anions, mostly Cl^-, out of the cell, thereby counteracting Donnan's effect. Thus, if the H^+ V-ATPase instead of the Na^+/K^+ P-ATPase plays the role of plasma membrane bioenergizer in renal ICs, then dissipation of the resting membrane potential and cell swelling are expected to occur after inhibition of the H^+ V-ATPase but not of the Na^+/K^+ P-ATPase. Therefore, we first tested the impact of blockade of either the H^+ V-ATPase or the Na^+/K^+ P-ATPase on the volume of β-ICs and principal cells in CCDs isolated from mouse kidney and superfused in vitro (18). We subsequently applied either 40 nM bafilomycinA1, a highly specific blocker of the H^+ V-ATPase (19), or 100 μM ouabain to block the Na^+/K^+ P-ATPase, and changes in cell volume were measured by monitoring the quenching of the fluorescent probe calcein using real-time two-photon imaging as described previously (20) (Movie S1). Application of bafilomycin A1 led to a significant increase in IC volume ($\Delta = +42 \pm 4\%$, $n = 12$), as evidenced by the quenching of calcein fluorescence. In line with our hypothesis, principal cell volume measured in the same tubules was unaffected by bafilomycin A1. Conversely, ouabain induced significant cell swelling of principal cells ($\Delta = +38 \pm 4\%$, $n = 9$), but not of ICs (Fig. 1 *A*–*C*).

We next assessed the impact of the H^+ V-ATPase on the resting potential of both intercalated and principal cells. Changes in membrane resting potential were monitored by measuring the quenching of fluorescence of the voltage-sensitive dye ANNINE-6, as previously described (21). Application of bafilomycin A1, as shown in Fig. 1 *D* and *E*, led to a significant depolarization of ICs ($\Delta = +34 \pm 2\%$, $n = 8$), indicating that the resting membrane potential in these cells critically depends on this pump. In contrast, bafilomycin A1 had no effect on the resting membrane potential of principal cells. Importantly, Muto et al. (22) have reported previously that blockade of the Na^+/K^+ P-ATPase by ouabain led to a marked depolarization of principal cells, but not of ICs. Taken together, these results indicate that the H^+ V-ATPase acts as a bioenergizer of IC's plasma membrane, whereas the Na^+/K^+ P-ATPase appears to be dispensable in this cell type.

NaCl Transepithelial Absorption by Renal ICs Is Energized by the H^+ V-ATPase but Not the Na^+/K^+ P-ATPase. One of the most prominent features of renal epithelial cells is their ability to mediate vectorial transepithelial NaCl transport. This process is dependent upon the activity of the Na^+/K^+ P-ATPase that converts the energy derived from metabolism into a steep inwardly directed sodium gradient. This sodium gradient energizes in turn numerous secondary or tertiary active transport systems. We recently examined transport properties of renal ICs on isolated renal tubules and identified an electroneutral thiazide-sensitive transport system in ICs (6). In these cells, NaCl absorption results from the functional coupling of the sodium-independent anion exchanger pendrin (Pds/Slc26a4) and of the sodium-dependent chloride/bicarbonate exchanger (Ndcbe) (Slc4a8).

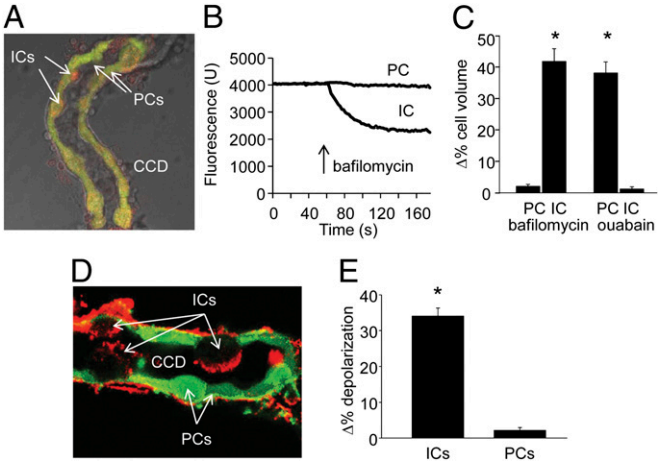

Fig. 1. Effects of inhibition of the H^+ V-ATPase on intercalated cell (IC) volume and membrane voltage in the isolated microperfused cortical collecting duct (CCD). (*A*) Cells were perfusion loaded with calcein-AM (green) and Alexa 594-conjugated peanut lectin (red) to identify ICs (red). A differential interference contrast overlay is shown. (*B*) Addition of 40 nM bafilomycin to the bathing solution caused a significant reduction of intracellular calcein fluorescence in ICs, indicating cell swelling, but not in principal cells (PCs). (*C*) Summary of bafilomycin or ouabain-induced cell volume changes in PCs vs. ICs. Ouabain (100 μM) was added to the bathing solution. $*P < 0.05$, IC or PC vs. baseline. (*D*) ANNINE-6 (green) was loaded from the bath; note its membrane-specific fluorescence along the basolateral cell membranes. The specific apical membrane binding of Alexa 594-conjugated peanut lectin (red) identified ICs. The image was taken in the presence of 40 nM bafilomycin in the bath. (*E*) In contrast to PCs that are intensely green fluorescent, ICs show diminished ANNINE-6 fluorescence indicating membrane depolarization. $*P < 0.05$, IC vs. baseline.

The luminal bicarbonate concentration in nephron segments expressing pendrin is expected to be very low due to avid reabsorption of bicarbonate in the proximal tubule and the loop of Henle. Hence, we assume that the bicarbonate required for sustaining NaCl absorption via ICs comes from active bicarbonate secretion by pendrin. Moreover, pendrin accumulates of chloride into the cells, which is expected to favor sodium and bicarbonate uptake via Ndcbe. Pendrin has been shown to be energized by an outwardly directed bicarbonate gradient, which results from primary active proton extrusion by the H^+ V-ATPase (23). Thus, we tested the dependence of transepithelial NaCl absorption on either the Na^+/K^+ P-ATPase or the H^+ V-ATPase. As indicated above, two distinct transport pathways account for Na^+ transepithelial absorption in the collecting duct: the first depends upon the epithelial sodium channel (ENaC), is electrogenic, amiloride-sensitive, and thiazide-resistant, and is located in the principal cells where it drives K^+ secretion (24); the second depends upon the parallel action of pendrin and the Na^+-driven Cl^-/HCO_3^- exchanger Ndcbe, is electroneutral, thiazide-sensitive, and amiloride-resistant, and is restricted to ICs (6). Inhibition of the Na^+/K^+ P-ATPase by 10^{-4} M ouabain abolished transepithelial voltage (V_{te}) and K^+ secretion in isolated microperfused mouse collecting ducts (Fig. 2 *A* and *B*). Similar effects were obtained by blocking the epithelial sodium channel ENaC of principal cells with 10^{-5} M amiloride. Application of both amiloride and ouabain (even at a concentration 10-fold higher) had no additional effects on V_{te} and K^+ secretion. Because V_{te} and K^+ secretion depend on the activity of the amiloride-sensitive Na^+ channel ENaC in principal cells (Fig. S1) and because ouabain had the same effects than 10^{-5} M amiloride, these experiments showed that 10^{-4} M ouabain is able to block ENaC-dependent Na^+ absorption completely. We

PHYSIOLOGY

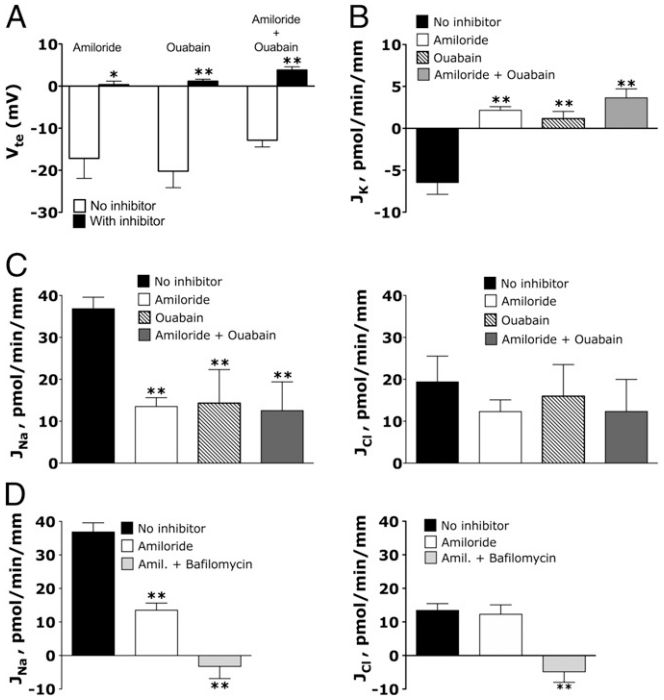

Fig. 2. Effects of amiloride (10^{-5} M), ouabain (10^{-4} M), and bafilomycin (4.0×10^{-8} M) on Na^+, Cl^-, K^+ transepithelial fluxes, and on transepithelial voltage (V_{te}) in CCDs isolated from Na^+-restricted mice. (*A*) CCDs isolated from mice on a Na^+-depleted diet develop a lumen negative V_{te}, which is completely abolished by either amiloride 10^{-5} M or ouabain at a concentration $\geq 10^{-4}$ M. (*B*) K^+ secretion is fully abolished by either amiloride 10^{-5} M or ouabain at a concentration $\geq 10^{-4}$ M. J_K, rate of K^+ secretion. (*C*) Na^+ absorption is inhibited by ~60% by either amiloride at 10^{-5} M or ouabain at 10^{-4} M, but the effects of the drugs are not additive indicating that the amiloride-resistant component of J_{na} is ouabain-resistant. Cl^- absorption is not affected by either amiloride at 10^{-5} M or ouabain at 10^{-4} M. (*D*) The amiloride-resistant component of NaCl absorption is abolished by addition of 10^{-8} M bafilomycin to the basolateral solution. n = 5–6 independent tubules per group. Statistical significance was tested by ANOVA followed by Bonferroni's post hoc test when appropriate. $^*P < 0.05$, and $^{**}P < 0.01$ vs. control (no inhibitor) group.

next assessed the effects of the same inhibitors on Na^+ and Cl^- absorption. Na^+ flux was only partially inhibited by either 10^{-5} M amiloride or 10^{-4} M ouabain (Fig. 2*C*). Again, the simultaneous application of both blockers did not lead to significant additive effects, demonstrating that ouabain alone is sufficient to block the amiloride-sensitive Na^+ absorption but does not affect amiloride-resistant Na^+ transport. In contrast, Cl^- transport was neither affected by application of amiloride, ouabain, nor simultaneous application of both compounds (Fig. 2*C*). We next tested the effects of 5×10^{-8} M bafilomycin A1 (19). Basolateral application of bafilomycin A1 fully inhibited the amiloride-resistant component of Na^+ and Cl^- absorption (Fig. 2*D*). These experiments demonstrate that sodium absorption by principal cells is primarily energized by the Na^+/K^+ P-ATPase, whereas sodium absorption by ICs might be exclusively energized by the H^+ V-ATPase.

Basolateral Na^+ Exit in β-ICs Occurs Through Ae4-Mediated Na^+-HCO_3^+ Cotransport. In epithelial cells, the Na^+/K^+ P-ATPase also provides a basolateral exit pathway for sodium. In the absence of the Na^+/K^+ P-ATPase, the parallel action of pendrin and Ndcbe energized by the H^+ V-ATPase is predicted to lead to net accumulation of Na^+ and HCO_3^- into the cell. Thus, we hypothesized that, in the nominal absence of the Na^+/K^+ P-ATPase, Na^+ transport across the basolateral membrane of ICs might be mediated by a bicarbonate-dependent sodium transporter energized by the H^+ V-ATPase.

We have previously reported that Ae4/Slc4a9 is specifically expressed in β-ICs (25). We also detected *Slc4a9* transcript by RT-PCR in cDNA of CCDs isolated from mouse kidney (Fig. S2). The localization and transport characteristics of Ae4/Slc4a9 are to some extent controversial. Concerning the different reported sites of Ae4 localization, previous studies lacked validation of the specificity of the Ae4 antibodies used on knockout tissue (26, 27). Even though Ae4 shares more similarities with Na^+-HCO_3^- cotransporters than with Cl^-/HCO_3^- exchangers of the SLC4 superfamily (28, 29), it has initially been cloned as a 4,4′-diisothiocyanatostilbene-2,2′-disulfonic acid (DIDS)-insensitive Na^+-independent Cl^-/HCO_3^- exchanger (27). Subsequently, Ae4 was reported to be rather DIDS sensitive (26). Finally, others reported that Ae4 might mediate Cl^--independent Na^+-HCO_3^- cotransport rather than Cl^-/HCO_3^- exchange (29, 30). To study the function of Ae4 function in vivo and to assess its potential role in Na^+ extrusion across the basolateral membrane of ICs, we disrupted *Slc4a9* in mice (Fig. S3). *Slc4a9*$^{-/-}$ mice from heterozygous matings followed Mendelian ratios and had no obvious phenotypical abnormalities. Anti-mouse Slc4a9 antibodies detected the presence of Ae4 in cells of the collecting duct from *Slc4a9*$^{+/+}$ mice by immunohistochemistry (Fig. 3 *A* and *B*). The staining was completely abolished in kidney sections from *Slc4a9*$^{-/-}$ mice demonstrating the specificity of the antisera generated (Fig. 3*C*). Ae4 labeling was exclusively detected at the basolateral membrane of renal epithelial cells that were identified as β-ICs because of apical expression of pendrin (Fig. 3 *D* and *E*). In contrast, α-ICs, which exhibit basolateral Ae1/Slc4a1 staining, were devoid of Ae4 labeling (Fig. 3*F*). The basolateral localization of Ae4 was further demonstrated by immunogold EM experiments (Fig. 3 *G* and *H*).

We also used a commercially available rabbit anti-human AE4 antibody (Alpha Diagnostics; catalog no. AE41-A) to examine Ae4 localization in CCDs isolated from rabbit kidney because apical localization of Ae4 has been previously reported in this species using an anti-rat Ae4 antibody (27). Fig. 4 *I–K* shows Ae4 labeling in a subpopulation of cells also stained with fluorescent peanut lectin, a marker of β-ICs in rabbit (31, 32). Moreover, colocalization studies of Ae4 with zona occludens protein 1 (ZO-1), a marker of the tight junction that delimits apical vs. lateral domains of epithelial cells, confirmed that, similar to mouse, Ae4 staining is restricted to the basolateral membrane of the cells (Fig. 3 *L* and *M*).

To study the role of Ae4 for NaCl reabsorption in its normal cellular context, CCDs dissected from the kidney of either *Slc4a9*$^{+/+}$ or *Slc4a9*$^{-/-}$ were microperfused in vitro as described (33). Subsequently, the effects of peritubular Na^+ removal or addition on IC's intracellular pH were measured. In CCDs isolated from *Slc4a9*$^{+/+}$ mice, removal of Na^+ from the peritubular solutions led to a marked intracellular acidification that was reversible upon restitution of Na^+ to the bath (Fig. 4 *A–C*). These Na^+-dependent changes of pH_i were not detected when tubules were perfused in CO_2/HCO_3^--free solutions, indicating that they reflect Na^+-coupled HCO_3^- fluxes and not Na^+/H^+ exchange. In CCDs isolated from *Slc4a9*$^{-/-}$ mice, Na^+-dependent pH_i changes were dramatically decreased independently of the presence of or absence of CO_2/HCO_3^-, which is in accordance with Na^+-dependent HCO_3^- fluxes mediated by Ae4. However, Slc4a9 deletion did not fully abolish the Na^+-dependent HCO_3^- fluxes, suggesting that another Na^+-HCO_3^- cotransporter coexists in the basolateral membrane of β-ICs (Fig. 4 *A–C*). We next analyzed whether Ae4 disruption blocks NaCl absorption by these cells. We have shown previously that NaCl absorption by ICs or principal cells can easily be distinguished since the former is amiloride resistant, whereas the latter is amiloride sensitive (6). CCDs isolated from *Slc4a9*$^{+/+}$ mice exhibited significant

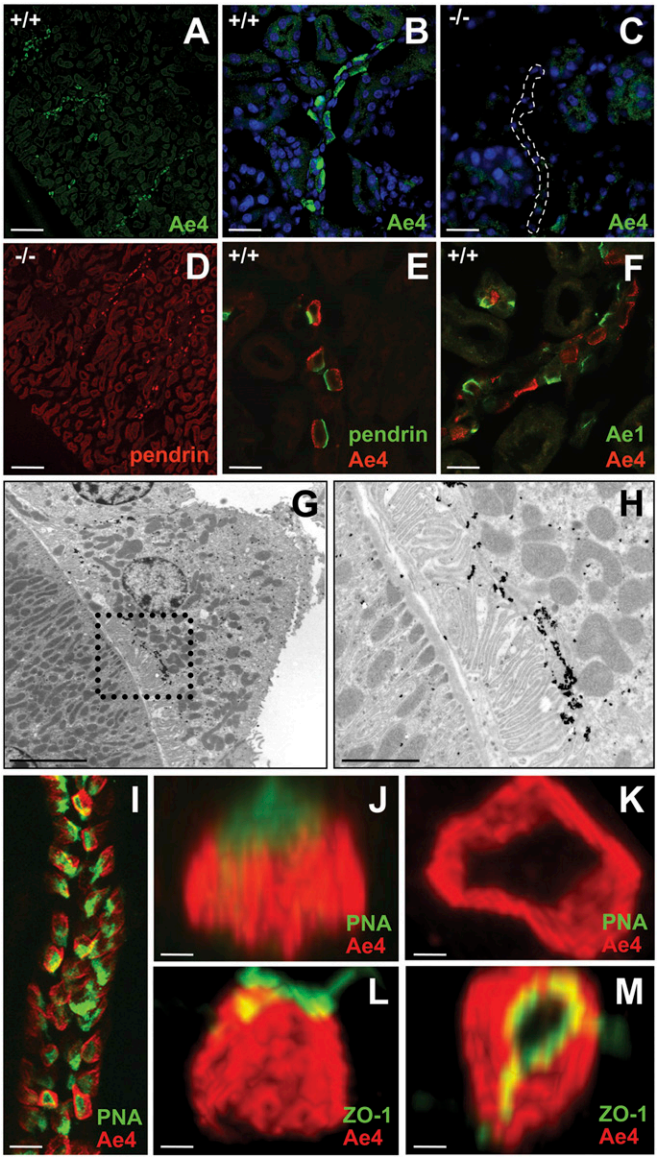

Fig. 3. Characterization of Slc4a9 (Ae4) expression. (*A* and *B*) Immunohistochemical detection of Slc4a9 (Ae4) protein abundance in the mouse kidney cortex using an anti-peptide antibody specific for the murine Slc4a9 protein in wild-type animals. (*A*) Low-magnification view of the whole renal cortex. (Scale bar, 200 μm.) (*B*) High-magnification view centered on a cortical collecting duct (CCD). (Scale bar, 40 μm.) (*C*) Absence of Slc4a9/Ae4 protein by immunohistochemistry in *Slc4a9*$^{-/-}$ mice. (Because of the absence of staining, the CCD is indicated by a dotted line.) (Scale bar, 40 μm.) (*D*) Localization of Slc26a4/pendrin (red) in the kidney cortex of *Slc4a9*$^{-/-}$ mice. (Scale bar, 20 μm.) (*E*) Localization of Slc26a4/pendrin (green) and Slc4a9/Ae4 (red) on opposite sides of type-B ICs in mice. (Scale bar, 20 μm.) (*F*) Localization of Slc4a1/Ae1 (green) and Slc4a9/Ae4 (red) within distal tubuli of the mouse kidney showing that AE1 and AE4 are expressed in different cells. (Scale bar, 40 μm.) (*G*) Immunogold labeling of mouse kidney sections with an anti-Ae4 antibody shows predominant basolateral staining, 3,000× magnification. (Scale bar, 5 μm.) (*H*) A 12,000× magnification of *Inset* in *G*. (Scale bar, 1 μm.) (*I*) CCDs microdissected from normal rabbit kidney were stained for Ae4 (red) and either peanut lectin (green in *I*, *J*, and *K*) or the tight junction protein ZO-1 (green in *L* and *M*). (Scale bar, 20 μm.) *I* reveals a *Z*-stack image of an individual CCD that was obtained via confocal microscopy. (Scale bar, 2 μm.) (*J*–*M*) Images are obtained via 3D reconstruction of individual β-ICs that have been rotated to view the lateral (*J* and *L*) and vertical (*K* and *M*) perspectives. (Scale bar, 2 μm.)

amiloride-resistant Na^+ and Cl^- absorption that was abolished in CCDs isolated from *Slc4a9*$^{-/-}$ mice (Fig. 4*D*). The effect in *Slc4a9*$^{-/-}$ mice was similar to that observed in *Slc4a8*$^{-/-}$ (Ndcbe) mice. Slc4a8 has previously been demonstrated to mediate the apical entry pathway for Na^+ in these cells (6) (Fig. 4*E*). Taken together, these experiments demonstrate that Ae4 mediates basolateral Na^+-HCO_3^- cotransport when expressed in its normal environment and that it mediates sodium extrusion from renal β-ICs.

Discussion

The present study provides evidence that mouse renal ICs, unlike most other animal cells, are not energized by the Na^+/K^+ P-ATPase, but rather are energized by the H^+ V-ATPase.

The presence of the Na^+/K^+ P-ATPase in renal ICs has been a matter of debate for almost 20 y. At least four independent studies failed to detect immunoreactivity for the Na^+/K^+ P-ATPase in either mouse or rat kidneys (34–37). A subsequent study using a strong antigen retrieval technique was able to demonstrate convincing staining of ICs with a set of different antibodies on rat kidney sections (38). However, the authors noticed that the staining was particularly weak in β-ICs of the renal cortex. Until recently, this was considered as evidence that ICs, in contrast to principal cells, can exclusively perform acid/base or chloride but not sodium or potassium transport. We recently challenged this concept by showing that ICs are able to absorb as much Na^+ as principal cells (6). The latter observation is puzzling if ICs have only few if not no Na^+/K^+ P-ATPase molecules. Indeed, this raised the question of the primary energy source required to support such a high Na^+ transport rate, and it was also unclear how Na^+ could exit the cell. Here, we show that the parallel action of the H^+ V-ATPase and of Ae4 mediates net Na^+ extrusion in a pH-neutral manner. Basolateral transport in ICs of Cl^- is likely to be mediated via ClC-KB/K2 (39–41), as these cells are also characterized by a very high Cl^- conductance (42). Due to the lack of an antibody to detect Ndcbe in the kidney by immunohistochemistry, we could not directly identify the subtype of ICs that exhibit thiazide-sensitive NaCl uptake. However, as this transport system requires pendrin, which is restricted to β-ICs, and because amiloride-resistant NaCl absorption was abolished by genetic ablation of Ae4, which is also exclusively expressed in β-ICs, most likely the β-ICs mediate this amiloride-resistant, thiazide-sensitive NaCl absorption.

The physiological role of electroneutral NaCl absorption by ICs remains unclear. In normal conditions, most of the NaCl reclamation in the aldosterone-sensitive distal nephron occurs in nephron segments located upstream to the CCD like the connecting tubule (CNT) (43) that also possess β-ICs, which are likely to be able to absorb NaCl as well. Under conditions of dietary sodium restriction, we observed that electroneutral NaCl absorption by ICs was stimulated (6). Supporting a physiological relevance of this system, a recent study demonstrated that the double deletion of both pendrin and NaCl cotransporter (NCC) in the distal convoluted tubule in mice leads to a marked salt-losing phenotype and early mortality (44), whereas the single deletion of each transporter has very mild consequences (45, 46). This suggests that NaCl absorption by ICs complements NCC and contributes to sodium balance regulation. Furthermore, NaCl absorption via the ICs is electroneutral and does affect K^+ transport, whereas ENaC-mediated Na^+ absorption drives K^+ secretion. Thus, it is tempting to speculate that this pathway might be particularly important when animals are volume contracted while at same time K^+ has to be spared.

Many different species, including *Xenopus laevis*, frog, fish, and insects comprise cell types that are functionally closely related to mammalian ICs, which are called chloride cells, ionocytes, or mitochondria-rich cells. Different studies have identified "chloride cells" from frog skin or fish gill as analogous to mammalian renal ICs. Interestingly, a recent study demonstrated that these

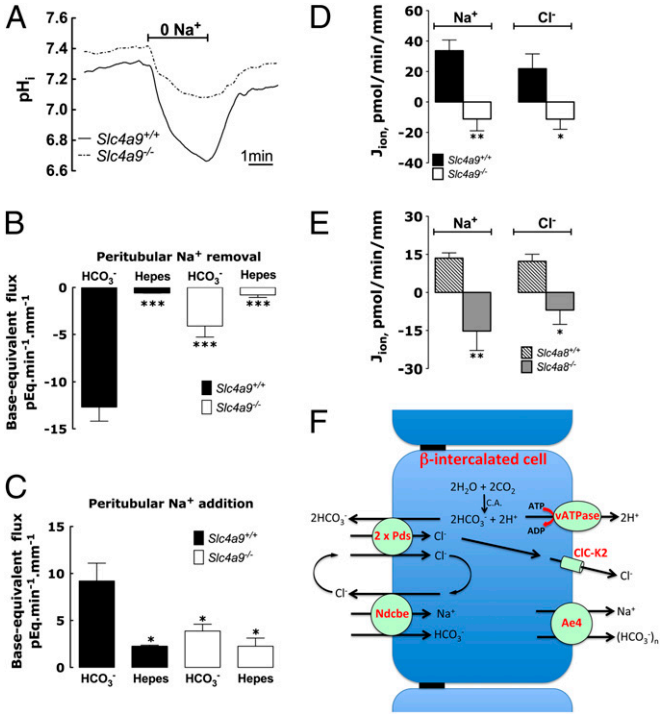

Fig. 4. Characterization of Ae4 activity in the mouse kidney. (*A*) Na^+ dependence of pH_i changes in ICs of CCDs isolated from *Slc4a9*$^{+/+}$ and *Slc4a9*$^{-/-}$ mice. In the experiments presented here, CCDs were isolated from mice fed on a Na^+-restricted diet. Traces shows the average of pH_i changes recorded in the presence of HCO_3^-/CO_2 when luminal Na^+ is initially removed from and then readded to the peritubular solution. Mean starting pH_i (immediately before luminal Na^+ removal) was 7.31 ± 0.05 in *Slc4a9*$^{+/+}$ mice in the presence of HCO_3^-/CO_2, 7.41 ± 0.12 in *Slc4a9*$^{-/-}$ mice in the presence of HCO_3^-/CO_2, 7.39 ± 0.10 in *Slc4a9*$^{+/+}$ mice in the absence of HCO_3^-/CO_2, and 7.38 ± 0.05 in *Slc4a9*$^{-/-}$ mice in the absence of HCO_3^-/CO_2, respectively. (*B* and *C*) Initial rates of base-equivalent fluxes during sodium removal (*B*) or addition (*C*) to the peritubular solutions in either the presence or the absence of HCO_3^-/CO_2. Values are means ± SE of values obtained in four to five independent ICs from three to six independent tubules; each tubule was isolated from independent animals. Statistical significance was tested by ANOVA followed by Bonferroni's post hoc test. *$P < 0.05$ and **$P < 0.01$ vs. all other groups. (*D*) Analyses of amiloride-resistant J_{Na}, and J_{Cl} in CCDs isolated from either *Slc4a9*$^{+/+}$ or *Slc4a9*$^{-/-}$ mice maintained on a Na^+-depleted diet. *$P < 0.05$, and **$P < 0.01$ vs. *Slc4a9*$^{+/+}$. Note that the magnitude of fluxes shown here cannot be compared with fluxes obtained in experiments shown in Fig. 2 or Fig. 4*E* because the Slc4a9 line has a different genetic background. (*E*) Analyses of amiloride-resistant J_{Na}, and J_{Cl} in CCDs isolated from either *Slc4a8*$^{+/+}$ or *Slc4a8*$^{-/-}$ maintained on a Na^+-depleted diet. *$P < 0.05$, and **$P < 0.01$ vs. *Slc4a8*$^{+/+}$. (*F*) Schematic description of electroneutral NaCl absorption energized by the H^+ V-ATPase. Two cycles of pendrin coupled with one cycle of Ndcbe result in the net uptake of one Na^+, one Cl^-, and two HCO_3^- ions, whereas one Cl^- ion is recycled across the apical membrane. Then Cl^- ion exits the cell through a basolateral chloride channel, while Na^+ and bicarbonate exit the cell at the basolateral membrane via Ae4. All these transporters are indirectly energized by the H^+ V-ATPase. C. A., carbonic anhydrase.

cells can be subdivided into two distinct subtypes with similar features as mammalian α- and β-ICs (47). Hence, we propose that the mode of energizing the cells described here might not be unique to mammalian renal ICs but may be applicable to related cells in other species. Indeed, previous studies have shown that proton transport in the mitochondria-rich cells of the turtle urinary bladder is tightly coupled to a large fraction of the metabolic energy of the cell (48). Even though our model for H^+ V-ATPase-dependent NaCl transepithelial transport (Fig. 4*F*) is based on results obtained in mouse and rabbit CCDs, we believe that it is applicable to a large number of epithelial cells characterized by plasma membrane expression of a H^+ V-ATPase in many different species.

Methods

A full detailed description of the methods can be found in *SI Full Methods*.

Ethic Statements. All animal protocols conformed to the "Protocol of Animal Welfare" (Amsterdam Treaty; www.eurocbc.org/page673.html) and were approved by the Institutional Animal Care and Use review board of Université Pierre et Marie Curie or of the University of Jena.

Microperfusion of Isolated CCDs. Experiments were performed as described previously in detail (6). Changes in pH_i were monitored using the pH-sensitive dye 2′,7′-bis-(2-carboxyethyl)-5-(and-6)-carboxyfluorescein (BCECF). ICs were distinguished from principal cells by their virtue of binding fluorescein-labeled peanut lectin [peanut agglutinin (PNA)] (Vector Labs) as described previously (6). For each tubule, three to four ICs were analyzed, and the mean gray level was measured with the Andor IQ software (Andor Technology). Ion fluxes on isolated CCDs were measured as previously described (6).

Generation of *Slc4a9* Knockout Mice. A fragment comprising exons 1–5 of the *Slc4a9* gene was isolated from a 129/SvJ mouse genomic λ library (Stratagene) to generate the targeting vector for homologous recombination. Genotyping was performed by analyzing genomic DNA from tail biopsies. Mice were genotyped either by Southern blot or by PCR.

Northern Analysis. Total RNA was isolated from various tissues of an adult C57BL/6 mouse using the RNeasy kit (Qiagen) according to the manufacturer's instructions. Ten micrograms of total RNA were separated by electrophoresis and blotted following standard protocols.

Slc4a9/Ae4-Antibody Generation. The Ae4 antisera were raised in rabbits against murine AE4 (GenBank accession no. NM_172830.2) with an N-terminal epitope KLPGQGDFESSDAHE(C) and a C-terminal epitope (C)PEEEETIPENRSEPE. The peptides were coupled via an N- or a C-terminal cysteine (in brackets) to KLH carrier. After immunopurification both antibodies gave consistent results in immunohistochemistry.

Immunostaining and EM of Kidney Sections or Isolated Tubules. Cryosections of 4% (mass/vol) paraformaldehyde-fixed tissues were labeled with antibodies directed against Slc4a1/Ae1 (1:1,000 from guinea pig; a gift from Carsten Wagner, Zurich), Slc26a4/pendrin (1:2,000 from guinea pig; a gift from Carsten Wagner), and Slc4a9/Ae4 (1:500 for immunohistochemistry and 1:1,000 for EM; see above) using standard protocols.

CCDs were microdissected from normal rabbit kidney and fixed in 1:4 dilution of Prefer concentrate (glyoxal fixative) in Dulbecco's PBS for 15 min (32). CCDs were then stained as previously described (32) with antibodies directed against Ae4 (rabbit anti-human AE4; Alpha Diagnostic International) or AE1:IV12 provided as a kind gift from M. L. Jennings (49) (University of Arkansas, Little Rock, AR). Colabeling was also performed with PNA-FITC (Vector Laboratories) or ZO-1, mouse monoclonal antibody-Alexa Fluor^{488} (catalog no. 339188; Invitrogen) was accomplished in a separate tertiary incubation. Three-dimensional reconstruction of individual ICs using the Fluoview software was performed to visualize the distribution of Ae4 in β-ICs and Ae1 in α-ICs.

Two-Photon Imaging and Semiquantitative Measurements of Changes in Cell Volume and Membrane Voltage in ICs. CCDs were isolated and perfused as described before (50). Cell volume was monitored using the cell volume marker calcein (Invitrogen) and cell voltage using ANNINE-6, a newly synthesized voltage-sensitive dye designed for ultrafast (1-ms) neural signal detection as described before (21). Preparations were visualized using a two-photon excitation laser scanning confocal fluorescence microscope (TCS SP2 AOBS MP confocal microscope system; Leica Microsystems). Images were collected in time series at 1 Hz and analyzed with the Leica LCS imaging software (LCS 2.61.1537) Quantification Tools. In some experiments, CCDs were preincubated with bafilomycin (40 nM) or ouabain (100 μM; both from Sigma). Each perfused CCD was dissected from a different animal.

ACKNOWLEDGMENTS. We thank Michael Schweizer (Zentrum für Molekulare Neurobiologie Hamburg) for support with the EM. D.E. and coworkers are supported by the Transatlantic Network for Hypertension from the Fondation Leducq, and by Agence Nationale de la Recherche Programme BLANC Grant 2010-R10164DD (to D.E.). J.P.-P. is funded by National

Institutes of Health (NIH) Grant DK64324. C.A.H. and I.K. are funded by the Deutsche Forschungsgemeinschaft. G.J.S. and J.M.P. are funded by NIH–National Institute of Diabetes and Digestive and Kidney Diseases Grant DK50603 (to G.J.S.).

1. Edelman IS (1974) Thyroid thermogenesis. *N Engl J Med* 290(23):1303–1308.
2. Izmail-Beigi F, Edelman IS (1970) Mechanism of thyroid calorigenesis: Role of active sodium transport. *Proc Natl Acad Sci USA* 67(2):1071–1078.
3. Asano Y, Liberman UA, Edelman IS (1976) Thyroid thermogenesis. Relationships between Na^+-dependent respiration and $Na^+ + K^+$-adenosine triphosphatase activity in rat skeletal muscle. *J Clin Invest* 57(2):368–379.
4. Morth JP, et al. (2011) A structural overview of the plasma membrane Na^+,K^+-ATPase and H^+-ATPase ion pumps. *Nat Rev Mol Cell Biol* 12(1):60–70.
5. Brown D, Breton S (1996) Mitochondria-rich, proton-secreting epithelial cells. *J Exp Biol* 199(Pt 11):2345–2358.
6. Leviel F, et al. (2010) The Na^+-dependent chloride-bicarbonate exchanger SLC4A8 mediates an electroneutral Na^+ reabsorption process in the renal cortical collecting ducts of mice. *J Clin Invest* 120(5):1627–1635.
7. Nelson N, Harvey WR (1999) Vacuolar and plasma membrane proton-adenosinetriphosphatases. *Physiol Rev* 79(2):361–385.
8. Nishi T, Forgac M (2002) The vacuolar (H^+)-ATPases—nature's most versatile proton pumps. *Nat Rev Mol Cell Biol* 3(2):94–103.
9. Pech V, et al. (2007) Angiotensin II increases chloride absorption in the cortical collecting duct in mice through a pendrin-dependent mechanism. *Am J Physiol Renal Physiol* 292(3):F914–F920.
10. Matsuzaki K, Stokes JB, Schuster VL (1989) Stimulation of Cl^- self exchange by intracellular HCO_3^- in rabbit cortical collecting duct. *Am J Physiol* 257(1 Pt 1):C94–C101.
11. Ehrenfeld J, Lacoste I, Harvey BJ (1989) The key role of the mitochondria-rich cell in Na^+ and H^+ transport across the frog skin epithelium. *Pflugers Arch* 414(1):59–67.
12. Wieczorek H, Brown D, Grinstein S, Ehrenfeld J, Harvey WR (1999) Animal plasma membrane energization by proton-motive V-ATPases. *Bioessays* 21(8):637–648.
13. Kriz W, Kaissling B (1985) Structural organization of the mammalian kidney. *The Kidney*, eds Seldin DW, Giebisch G (Raven, New York), pp 265–306.
14. Purkerson JM, Schwartz GJ (2007) The role of carbonic anhydrases in renal physiology. *Kidney Int* 71(2):103–115.
15. Hennings JC, et al. (2012) A mouse model for distal renal tubular acidosis reveals a previously unrecognized role of the V-ATPase a4 subunit in the proximal tubule. *EMBO Mol Med* 4(10):1057–1071.
16. Royaux IE, et al. (2001) Pendrin, encoded by the Pendred syndrome gene, resides in the apical region of renal intercalated cells and mediates bicarbonate secretion. *Proc Natl Acad Sci USA* 98(7):4221–4226.
17. Alper SL, Natale J, Gluck S, Lodish HF, Brown D (1989) Subtypes of intercalated cells in rat kidney collecting duct defined by antibodies against erythroid band 3 and renal vacuolar H^+-ATPase. *Proc Natl Acad Sci USA* 86(14):5429–5433.
18. Peti-Peterdi J, et al. (2000) Macula densa Na^+/H^+ exchange activities mediated by apical NHE2 and basolateral NHE4 isoforms. *Am J Physiol Renal Physiol* 278(3): F452–F463.
19. Bowman EJ, Siebers A, Altendorf K (1988) Bafilomycins: A class of inhibitors of membrane ATPases from microorganisms, animal cells, and plant cells. *Proc Natl Acad Sci USA* 85(21):7972–7976.
20. Liu R, Persson AE (2005) Simultaneous changes of cell volume and cytosolic calcium concentration in macula densa cells caused by alterations of luminal NaCl concentration. *J Physiol* 563(Pt 3):895–901.
21. Marsh DJ, Toma I, Sosnovtseva OV, Peti-Peterdi J, Holstein-Rathlou NH (2009) Electrotonic vascular signal conduction and nephron synchronization. *Am J Physiol Renal Physiol* 296(4):F751–F761.
22. Muto S, Imai M, Asano Y (1993) Further electrophysiological characterization of the alpha- and beta-intercalated cells along the rabbit distal nephron segments: Effects of inhibitors. *Exp Nephrol* 1(5):301–308.
23. Tsuruoka S, Schwartz GJ (1999) Mechanisms of HCO_3^- secretion in the rabbit connecting segment. *Am J Physiol* 277(4 Pt 2):F567–F574.
24. Garty H, Palmer LG (1997) Epithelial sodium channels: Function, structure, and regulation. *Physiol Rev* 77(2):359–396.
25. Hentschke M, Hentschke S, Borgmeyer U, Hübner CA, Kurth I (2009) The murine AE4 promoter predominantly drives type B intercalated cell specific transcription. *Histochem Cell Biol* 132(4):405–412.
26. Ko SB, et al. (2002) AE4 is a DIDS-sensitive Cl^-/HCO_3^- exchanger in the basolateral membrane of the renal CCD and the SMG duct. *Am J Physiol Cell Physiol* 283(4): C1206–C1218.
27. Tsuganezawa H, et al. (2001) A new member of the HCO_3^- transporter superfamily is an apical anion exchanger of beta-intercalated cells in the kidney. *J Biol Chem* 276(11):8180–8189.
28. Lipovich L, Lynch ED, Lee MK, King MC (2001) A novel sodium bicarbonate cotransporter-like gene in an ancient duplicated region: SLC4A9 at 5q31. *Genome Biol* 2(4):Research/0011.0011–Research/0011.0013.
29. Romero MF, Fulton CM, Boron WF (2004) The SLC4 family of HCO_3^- transporters. *Pflugers Arch* 447(5):495–509.
30. Parker MD, Tanner MJA, Boron WF (2002) Characterization of human AE4 as an electroneutral, sodium-dependent bicarbonate transporter. *FASEB J* 16:A796.
31. Schuster VL, Bonsib SM, Jennings ML (1986) Two types of collecting duct mitochondria-rich (intercalated) cells: Lectin and band 3 cytochemistry. *Am J Physiol* 251(3 Pt 1): C347–C355.
32. Schwartz GJ, et al. (2002) Acid incubation reverses the polarity of intercalated cell transporters, an effect mediated by hensin. *J Clin Invest* 109(1):89–99.
33. Burg M, Grantham J, Abramow M, Orloff J (1966) Preparation and study of fragments of single rabbit nephrons. *Am J Physiol* 210(6):1293–1298.
34. Kashgarian M, Biemesderfer D, Caplan M, Forbush B, 3rd (1985) Monoclonal antibody to Na,K-ATPase: Immunocytochemical localization along nephron segments. *Kidney Int* 28(6):899–913.
35. Holthöfer H, Schulte BA, Pasternack G, Siegel GJ, Spicer SS (1987) Three distinct cell populations in rat kidney collecting duct. *Am J Physiol* 253(2 Pt 1):C323–C328.
36. Piepenhagen PA, Peters LL, Lux SE, Nelson WJ (1995) Differential expression of Na^+-K^+-ATPase, ankyrin, fodrin, and E-cadherin along the kidney nephron. *Am J Physiol* 269(6 Pt 1):C1417–C1432.
37. Buffin-Meyer B, et al. (1998) Regulation of Na^+, K^+-ATPase in the rat outer medullary collecting duct during potassium depletion. *J Am Soc Nephrol* 9(4):538–550.
38. Sabolić I, Herak-Kramberger CM, Breton S, Brown D (1999) Na/K-ATPase in intercalated cells along the rat nephron revealed by antigen retrieval. *J Am Soc Nephrol* 10(5):913–922.
39. Estévez R, et al. (2001) Barttin is a Cl^- channel beta-subunit crucial for renal Cl^- reabsorption and inner ear K^+ secretion. *Nature* 414(6863):558–561.
40. Kieferle S, Fong P, Bens M, Vandewalle A, Jentsch TJ (1994) Two highly homologous members of the ClC chloride channel family in both rat and human kidney. *Proc Natl Acad Sci USA* 91(15):6943–6947.
41. Nissant A, Paulais M, Lachheb S, Lourdel S, Teulon J (2006) Similar chloride channels in the connecting tubule and cortical collecting duct of the mouse kidney. *Am J Physiol Renal Physiol* 290(6):F1421–F1429.
42. Muto S, Yasoshima K, Yoshitomi K, Imai M, Asano Y (1990) Electrophysiological identification of alpha- and beta-intercalated cells and their distribution along the rabbit distal nephron segments. *J Clin Invest* 86(6):1829–1839.
43. Christensen BM, et al. (2010) Sodium and potassium balance depends on αENaC expression in connecting tubule. *J Am Soc Nephrol* 21(11):1942–1951.
44. Soleimani M, et al. (2012) Double knockout of pendrin and Na-Cl cotransporter (NCC) causes severe salt wasting, volume depletion, and renal failure. *Proc Natl Acad Sci USA* 109(33):13368–13373.
45. Schultheis PJ, et al. (1998) Phenotype resembling Gitelman's syndrome in mice lacking the apical Na^+-Cl^- cotransporter of the distal convoluted tubule. *J Biol Chem* 273(44): 29150–29155.
46. Verlander JW, et al. (2003) Deoxycorticosterone upregulates PDS (Slc26a4) in mouse kidney: Role of pendrin in mineralocorticoid-induced hypertension. *Hypertension* 42(3):356–362.
47. Quigley IK, Stubbs JL, Kintner C (2011) Specification of ion transport cells in the *Xenopus* larval skin. *Development* 138(4):705–714.
48. Beauwens R, Al-Awqati Q (1976) Active H^+ transport in the turtle urinary bladder. Coupling of transport to glucose oxidation. *J Gen Physiol* 68(4):421–439.
49. Jennings ML, Anderson MP, Monaghan R (1986) Monoclonal antibodies against human erythrocyte band 3 protein. Localization of proteolytic cleavage sites and stilbenedisulfonate-binding lysine residues. *J Biol Chem* 261(19):9002–9010.
50. Sipos A, et al. (2009) Connexin 30 deficiency impairs renal tubular ATP release and pressure natriuresis. *J Am Soc Nephrol* 20(8):1724–1732.